J Paleolimnol (2008) 39:17–33
DOI 10.1007/s10933-007-9092-3

ORIGINAL PAPER

Isotopic evolution and climate paleorecords: modeling boundary effects in groundwater-dominated lakes

Mark D. Shapley · Emi Ito · Joseph J. Donovan

Received: 23 June 2006 / Accepted: 23 January 2007 / Published online: 6 April 2007

Abstract We used an isotopic mass-balance model to examine how the hydrogeologic setting of lakes influences isotopic response of evaporating lake water to idealized hydroclimatic changes. The model uses a monthly water and isotope balance approach with simplified water-column structure and groundwater exchanges. The framework for comparative simulations is provided by lakes in a region of the Northern Rocky Mountains that display high interlake geochemical variability, thought to be controlled by groundwater hydraulics. Our analysis highlights several isotopic effects of flow between aquifers and lakes, leading to possible divergence of isotopic paleorecords formed under a common climate. Amplitude of isotopic variation resulting from simulated climate forcing was greatly damped when high groundwater fluxes and/or low lake volume resulted in low lake fluid residence time. Differing precipitation and evaporation scenarios that are equivalent in annual fluid balance (P–E) resulted in different isotopic signatures, interpreted as a result of evaporation kinetics. Concentrating low-δ groundwater inflow during spring months raised springtime lake δ values, a counterintuitive result of coincidence between times of high groundwater inflow and the evaporation season. Transient effects of reduced fluid balance caused excursions opposite in sign from eventual steady-state isotopic shifts resulting from enhanced groundwater inflow dominance. Lags in response between climate forcing and isotopic signals were shortened by high groundwater fluxes and resulting short lake residence times. Groundwater-lake exchange exerts control over patterns of lake isotopic response to evaporation through effects on lake residence time, inflow composition, and seasonal timing of inflow and outflow. Sediments from groundwater-linked lakes, often used for paleoenvironmental analysis, should be expected to reflect isotopic complexities of the type shown here.

Keywords Lakes · Groundwater · Oxygen isotopes · Evaporative evolution · Isotope modeling · Isotope hydrology · Climate · Ovando Valley · Montana

Electronic supplementary material The online version of this article (doi:10.1007/s10933-007-9092-3) contains supplementary material, which is available to authorized users.

M. D. Shapley (✉) · E. Ito
Limnological Research Center, Department of Geology and Geophysics, University of Minnesota, 310 Pillsbury Drive SE., Minneapolis, MN 55455, USA
e-mail: shap0029@umn.edu

J. J. Donovan
Department of Geology and Geography, West Virginia University, 425 White Hall, Morgantown, WV 26506, USA

Introduction

Fluid exchange between groundwater and lakes influences lake geochemistry, both through the composition of groundwater inflow and through control over lake residence time. Where the ratio of groundwater inflow to surface water inflow is high, lakes can be referred to as groundwater-dominated (Born et al. 1979; Donovan 1992). As in other lake types, composition and accumulation rates of endogenic (sensu Last 2001) carbonate minerals are among the most direct measures available of paleolake hydrologic status (e.g. Dean and Stuiver 1993; Benson et al. 1996; Ito 2001). Groundwater processes may, however, result in lake geochemical response different from that seen in lakes where groundwater fluxes are unimportant. In particular, effects of aquifer hydraulics on lake residence time can lead to contrasting compositional evolution of lakes within a common climatic regime (Krabbenhoft et al. 1990; Sanford and Wood 1991; Donovan 1994; Gosselin et al. 1997; Walker and Krabbenhoft 1998; Shapley et al. 2005). Transient groundwater effects translate into differential lake geochemical response to evaporative forcing, controlled by aquifer hydraulics and lake morphometry (Donovan 1994). Sensitivity of ionic composition and environmental isotopes to lake/groundwater exchange can differ, leading to apparent discrepancies between trends in salinity and isotopic composition (Gosselin et al. 1997; Smith et al. 1997; Donovan et al. 2002; Dean et al. 2002; Yu et al. 2002). As a consequence, interpretation of the environmental paleorecords commonly extracted from such lake systems may be confounded. Further complicating effects of groundwater exchange rates may arise with attempts to reconstruct nutrient fluxes (Schettler et al. 2006) and even in the establishment of sediment chronologies (Brenner et al. 2006).

Groundwater relationships can have a strong effect on the mean isotopic composition of lake water (Fig. 1), which will be translated into sedimentary records of isotopic change. We suggest that hydrogeology, through effects on residence time, inflow timing and source compositional mix, will further modulate the isotopic expression of climate signals in ways that affect the apparent magnitude, timing and interlake coherence of lake paleorecord signals. Here we examine this influence, using an isotope mass-balance model to analyze lake isotopic sensitivity to changes in fluid balance under contrasting groundwater boundary conditions. Modern field observations from groundwater-dominated lakes of the Ovando Valley, Montana (Fig. 2) are used for comparison to model results, providing illustrative boundary conditions and a field context for model observations.

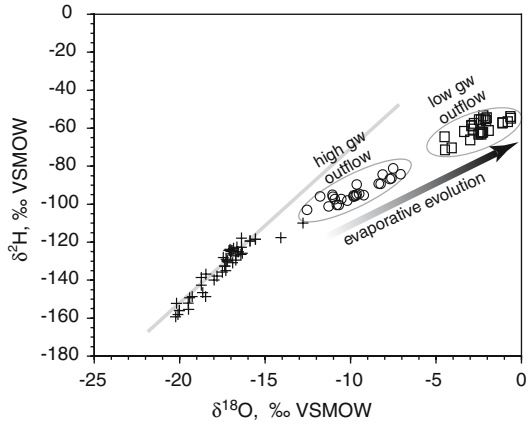

Fig. 1 Groundwater interactions can have large effects on the evolution of lake isotopic composition under evaporative conditions. Here two groundwater-dominated lakes in a common climatic regime express strongly contrasting compositions evolved from similar source compositions. The two lakes are hydrologically distinguished by very different groundwater outflow rates, governed by topography and permeability of lake-basin geologic materials

Field setting and methods

The geologic and hydroclimatic settings of the Ovando Valley are described in detail elsewhere (Shapley et al. 2005). In brief, numerous lakes and wetlands occupy topographically closed depressions within a complex of late-glacial ice-contact and glaciofluvial sediments (Dea 1981). Highly heterogeneous ionic chemistry is governed primarily by hydraulic controls over lake/aquifer fluid fluxes and resulting contrasts in lake fluid residence time (Shapley et al. 2005). Lake geochemical response to regional hydroclimatic forcing is thereby recorded differentially

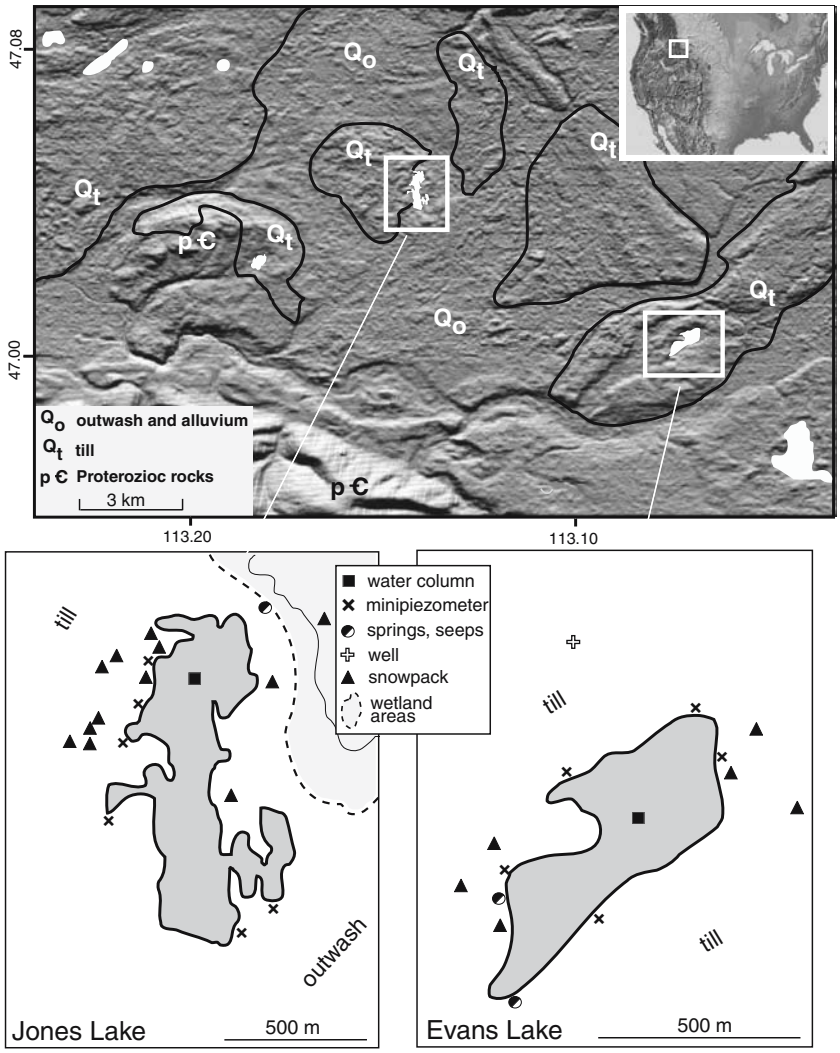

Fig. 2 Field location and sampling sites at Jones and Evans lakes, Ovando Valley (US). Regional groundwater flow is generally southward, discharging to the Blackfoot River. Local groundwater inflow to Jones Lake occurs from the west and south; wetland area NE of Jones Lake receives copious groundwater outflow supplied by lake seepage through permeable late Glacial sediments. Inflow to Evans Lake occurs from the north, west and south

across the landscape, according to relationships between groundwater inflow and outflow rates.

Water sampling and analysis

Field data were compiled from sampling of lake waters across the Ovando Valley as well as serial sampling from 1998 to 2002 (approximately quarterly) of two primary research sites, Evans Lake and Jones Lake (Table 1). Lake and wetland samples were collected either by Van Dorn bottle or by peristaltic pumping from measured lake depths. Shallow groundwater was sampled through minipiezometer (Winter et al. 1988) installations in littoral sediments and by grab sampling of springs and seeps at their most upstream point of discharge. Deeper groundwater was sampled from water supply wells. Streams receiving groundwater discharge were sampled under autumn baseflow conditions.

Composited snow was sampled in late March (near the time of maximum snow-water storage) by driving a clean polycarbonate cylinder completely through the snowpack. About 3–15 snow plugs per sampling site were aggregated, melted isothermally at 0°C, and subsampled for stable isotope analyses. Occasional samples of rain events were collected in a sealed reservoir equipped with a vapor lock. Water samples were collected in either 20 ml HDPE bottles with conical Teflon^{TM} cap inserts, or crimp-sealed in 20 ml glass serum vials. Analysis of water samples

Table 1 Summary data for Evans Lake and Jones Lake field sites after which modeling experiments are structured

	Evans Lake	Jones Lake
Surface elevation, 8/2000	1279.9 m (MSL)	1248.3 m (MSL)
Surface area, 8/2000	2.57 E5 m^2	3.22 E5 m^2
Maximum depth, 8/2000	7.7 m	12.5 m
Mean depth, 8/2000	2.37 m	2.46 m
Volume, 8/2000	6.08 E5 m^3	7.84 E5 m^3
Observed TDS range	~9,500–13,300 mg/l	~150–350 mg/l
Hydraulic residence time	8–9 years	1.5–2 years

Residence time estimates are based on steady-state solute balance calculations. Comprehensive geochemical data can be found in Shapley et al. (2005)

occurred either at the University of Minnesota Stable Isotope Laboratory (MSIL) or at the University of Arizona Stable Isotope Laboratory (ASIL). Oxygen samples analyzed at the MSIL were manually extracted by CO_2 equilibration (Epstein and Mayeda 1953). Hydrogen samples analyzed at the MSIL were manually extracted to hydrogen gas by zinc catalysis (Kendall and Coplen 1985). MSIL samples were analyzed on a Finnigan-MAT Delta E multi-collector, dual inlet isotope ratio mass spectrometer with analytical precision of 0.1‰ for $\delta^{18}O$ and 1‰ for δ^2H. ASIL samples were extracted on an automated system by CO_2 equilibration (oxygen) and by chromium catalysis (hydrogen) and analyzed on a Finnigan Delta S instrument with analytical precision of 0.08‰ and 0.9‰ respectively.

Lake basin hypsometry

Isotopic evolution of evaporating water bodies depends strongly on ratios of fluid fluxes (Gat 1995), which in turn are influenced by lake-basin morphometry. Morphometric models of the Evans Lake and Jones Lake watersheds were developed by a combination of acoustic profiling of lake depth cross sections, 1:24,000 Digital Orthophoto Quad (DOQ) imagery of lake basins, and manual surveying. Digital cross sections generated from acoustic profiles were scaled to the DOQ images. The resulting xyz files were converted to 3-m grids of lake bottom/land surface elevation with an isotropic point kriging scheme. Depth/area/volume relationships for the two lakes were then calculated using standard Surfer 7™ tools. On the basis of comparison with measured depths, volumetric errors in the models at all but very low lake volumes are estimated to be no more than ± 5%.

Isotope balance model structure and development

The model developed to examine lake isotopic sensitivity is coded in VisualBasic for Excel™ and incorporates groundwater exchange, evaporation and precipitation fluxes, and seasonal lake stratification. (See code and explanation of variables as ESM 1.) Model structure is adapted from that of Benson and Paillet (2002). Monthly fluid fluxes are used to calculate changes in lake volume as

$$\begin{aligned} VOL_{LAKE(n)} = \; & VOL_{LAKE(n-1)} + VOL_{PPT(n)} \\ & + VOL_{GWIN(n)} - VOL_{EVAP(n)} \\ & - VOL_{GWOUT(n)} \end{aligned} \quad (1)$$

and monthly isotopic change calculated as

$$\begin{aligned} \Delta\delta_{LAKE(n)} = \; & [(\delta_{GWIN(n)} * VOL_{GWIN(n)}) \\ & + (\delta_{PPT(n)} * VOL_{PPT(n)}) \\ & - (\delta_{LAKE(n-1)} * VOL_{GWOUT(n)}) \\ & - (\delta_{EVAP(n)} * VOL_{EVAP(n)}) \\ & - (\delta_{LAKE(n-1)} * \delta VOL_{LAKE(n)})]/ \\ & VOL_{LAKE(n)} \end{aligned} \quad (2)$$

where $VOL_{(LAKE)}$ = lake volume, m^3: VOL_{PPT} = monthly on-lake precipitation, m^3: VOL_{EVAP} = monthly lake evaporation, m^3: VOL_{GWIN} = monthly groundwater inflow, m^3: VOL_{GWOUT} = monthly groundwater outflow, m^3: n = month and subscripted δ represents the $\delta^{18}O$ and δ^2H composition of each monthly flux in standard notation relative to VSMOW.

Ovando-area environmental parameters and lake observations provide a convenient modeling framework for examining the influence of groundwater boundaries on lake evolution. Monthly lake surface areas are determined from

lake volume and interpolated lake hypsometric matrices. Annual precipitation, monthly precipitation distribution and monthly average air temperature (Table 2) were taken from summary data for the Ovando climate station (NWS station 246302; period of record 1899–1976). Relative humidity (RH) estimates were drawn from a Montana Department of Transportation Remote Weather Information System (RWIS) instrument array located 5 km east of Evans Lake (http://www.mdt.mt.gov/travinfo/weather/rwis.shtml). Precipitation compositions were drawn from the monthly interpolations of Bowen and Revenaugh (2003). Base case groundwater inflow rates were derived from solute balance analyses (Shapley et al. 2005). Modeled groundwater outflow is assumed to be linearly related to lake volume above a threshold, zero-discharge volume, following the approach of Donovan (1992). Exponential stage–volume relationships of the hypsometric models result in arbitrary but physically plausible nonlinear relations between outflow and lake stage. Monthly evaporation rates were specified on the basis of regionalized Penman calculations (MAPS 2003), which are generally consistent with the limited local evaporation pan data (Cook 2001). Model evaporation does not occur during the months November–March, normally the minimum duration of seasonal ice cover. The model incorporates direct precipitation into lake volume changes throughout the year, inducing artificial continuity in lake fluxes during seasons of snow accumulation. Monthly lake mixing depth is specified empirically based on limited observations from 1998 to 2003 (Shapley et al. 2005); the model does not incorporate heat storage or other buoyancy terms. Interannual hydroclimatic variability is simulated using sinusoidal and step-function changes imposed on the three hydroclimatic boundary conditions (precipitation rate, evaporation rate, and groundwater inflow rate) treated as independent variables.

$\delta^{18}O$ and $\delta^{2}H$ values of evaporated water vapor are calculated according to equilibrium fractionation equations of Majoube (1971) and kinetic fractionation equations of Gonfiantini (1986). The model is formulated with two alternative fractionation routines. One employs an explicit advected vapor factor (Benson and Paillet 2002); the other routine uses Gonfiantini's earlier equations, implicitly assuming all vapor overlying the modeled lake surface to be advected. Gonfiantini's formulation ignores the effects of lake evaporation on the overlying vapor composition. The experiments described here used the Gonfiantini approximation because model trials with the explicit advected factor showed unrealistically low sensitivity of the simulated lake $\delta^{18}O$:$\delta^{2}H$ relationship (the evaporation trend) to RH. The errors resulting from the 100% advected vapor assumption are probably modest in the case of the small lakes discussed here, and are unlikely to effect the conclusions of this analysis.

Table 2 Monthly model assumptions common to all simulations

Month	$\delta^{18}O_{GWIN}$	$\delta^{18}O_{PPT}$	Air temp	Rel hum %	Water temp JL/EL	Strat depth JL/EL
Jan	–16.7	–20.35	–3.8	71	3/0.5	0/0
Feb	–16.7	–18.98	–2.2	59	3/0.5	0/0
Mar	–16.7	–16.99	–0.4	51	3/2	0/0
Apr	–16.7	–13.83	3.8	40	6/5	1/1
May	–16.7	–10.87	8.2	39	10.5/11	2.5/2.5
Jun	–16.7	–10.65	12.2	40	17/17.5	3/3
Jul	–16.7	–9.87	18.9	32	22/23	3.5/3.5
Aug	–16.7	–10.8	18.2	30	22.5/23.5	4/4
Sept	–16.7	–11.02	11.8	35	17/17.5	5.5/5.5
Oct	–16.7	–12.57	5.4	42	7.5/7	0/0
Nov	–16.7	–16.88	0.0	64	4/3	0/0
Dec	–16.7	–19.28	–2.6	72	3/1	0/0

See ESM 1 for complete list of model variables

Field results

Lake compositions

Sampled Ovando-area lakes and wetlands (ESM 2) range from –16.8‰ to +3.9‰ VSMOW in δ^{18}O (–123‰ to –25‰ in δ^{2}H). Compositions fall along a well-defined evaporation trend with a slope of 4.6 and separation of about 7‰ between Jones Lake and Evans Lake mean δ^{18}O values (Fig. 3).

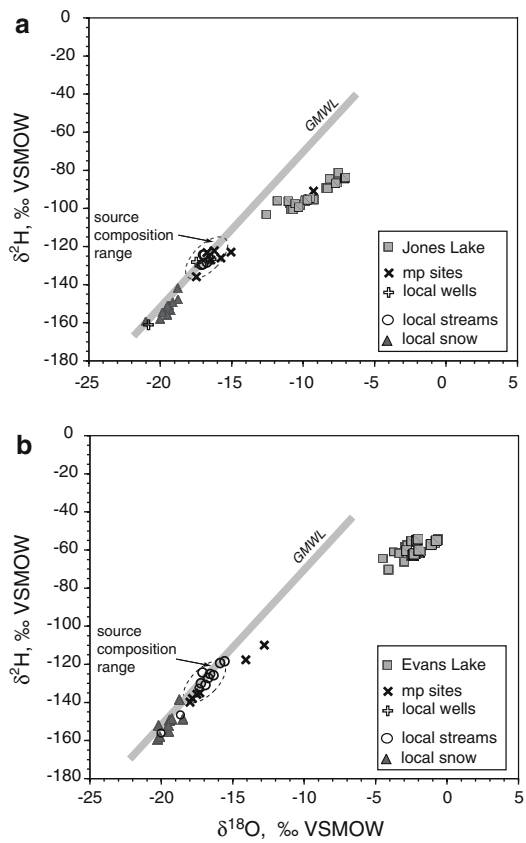

Fig. 3 Field compositions (1997–2002) and inferred source compositions for (**a**) Jones Lake (**b**) Evans Lake. Inferred source compositions are determined by the intersection of local evaporation and meteoric trends. Dashed ovals represent estimates of the uncertainty in weighted mean source composition for each lake. GMWL represents the 'global meteoric water line' of $\delta^{2}H = 8.13*\delta^{18}O + 10.8$. Stream compositions reflect grab samples from turbulent mid-stream sites. Snow compositions are for composited cores of entire snowpack. Inferred source compositions correspond closely to shallow groundwater sampled by minipiezometer. (Shallow groundwater samples falling below the GMWL show ionic compositions indicative of lake water reflux)

In Jones Lake, δ^{18}O values ranged seasonally from –12‰ to –7‰. Data for Evans Lake for the same period show that mixed-layer waters varied seasonally over a 1.5‰–3‰ range in δ^{18}O and over a 4‰ range (–4.5‰ to –0.5‰ VSMOW) during the course of the sampling. Hypolimnetic δ^{18}O values varied between –3‰ and –1‰. Mixed layer δ^{18}O values showed an increasing trend reaching about 2.5‰over the period of record.

Composition of lake inflow

Jones and Evans lakes receive inflow primarily from local groundwater and direct on-lake precipitation; outflows are by groundwater seepage and evaporation. Well water, snow and groundwater-derived stream baseflow suggest a regional meteoric δ^{18}O:δ^{2}H trend closely following the global meteoric water line (GMWL; Fig. 3).

The intercept of the evaporation and meteoric trends implies an approximate weighted source composition from which lake isotopes evolve (Gat 1995). Here the lake trends intersect the GMWL near δ^{18}O and δ^{2}H compositions of –16.7‰ and –126‰, respectively. This inferred source composition is very near both the local mean minipiezometer composition at each lake (excepting 3 samples affected by lake-water seepage) and the mean composition of nearby stream baseflow. Inferred and sampled source compositions are thus in close agreement and indistinguishable between the two lakes.

Relation to interpolated North American data sets

Using the IAEA global precipitation data set, Bowen and Revenaugh (2003) developed a model of global precipitation composition coupling an empirical latitude and elevation function with station-based interpolation of the residual variance in δ values. Here we use their mean monthly estimates for the latitude, longitude and elevation of Jones Lake (http://ecophys.biology.utahedu/LabFolks/gbowen/pages/OIPC_Main.html). Due to the lack of nearby IAEA monitoring, the standard error of monthly δ^{18}O estimates could be large (several ‰). Nonetheless, within the limits of uncertainty, Bowen and Revenaugh's

model produces results consistent with our field data. Averaged mean monthly estimates for the period of snow accumulation are near –19‰ in δ^{18}O. Unweighted mean composition of mature, near-isothermal snowpack in our data set is –19.3‰. Estimated monthly mean δ^{18}O values for May and June, when most summer rain occurs, are –10.9‰ and –10.0‰. Our few summer rainfall samples, which represent partial sampling of convective storms, range from –8.2‰ to –6.7‰.

Lake source compositions inferred from evaporation trends and groundwater compositions are about 2.2‰ lower in δ^{18}O values than estimates of weighted mean annual precipitation from Bowen and Revenaugh's model (δ^{18}O = –14.3‰; δ^{2}H = –108‰). This reflects expected bias in the seasonality of groundwater recharge, favoring infiltration of snowmelt and cool season rain over summer (growing season) precipitation.

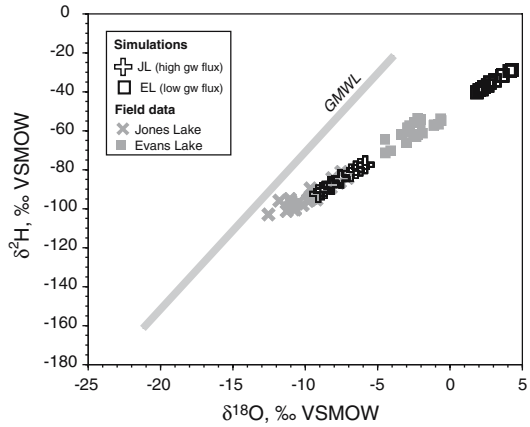

Fig. 4 Base case model compositions under seasonally varying steady-state conditions, with lake field data for comparison. Initial conditions are based on fluid fluxes calculated from solute balance (Shapley et al. 2005) and lake composition identical to groundwater inflow. Steady-state model results closely follow field compositions in slope and annual range of δ^{18}O values but exceed mean δ values of Jones and Evans lakes

Modeling results and interpretation

General model behavior

The model described here is intended as a tool for examining concepts of isotopic exchange between lakes and groundwater. Although structured around observed lake and groundwater relationships, we do not propose the result as a calibrated representation of Ovando lake geochemistry, which would require better constraint of several variables influencing both composition and rate of evaporation. Nevertheless, comparisons to field observations help demonstrate the value and limitations of our modeling analyses. Simulations of the high-groundwater flux system (analogous to Jones Lake) are referred to as JL, while simulations of the restricted-flux system (modeled after Evans Lake) are referred to as EL. Proper lake names are reserved for reference to field observations.

Simulated monthly lake compositions under the base case model climatology (Table 2) are shown in Fig. 4. The departure of the evaporation trend from the meteoric water line reflects the diffusion-controlled kinetic fractionation of water molecules during vapor–liquid exchange (Craig and Gordon 1965; Merlivat and Jouzel 1979). Sensitivity of the evaporation slope is primarily to RH (Majoube 1971; Merlivat and Jouzel 1979), with convergence on the meteoric water line at RH near 100%. Modeled pathways of isotopic evolution under a range of monthly humidity distributions show the model sensitivity to RH is qualitatively correct; however field values of RH initially tested (RWIS monthly medians for daylight hours) underestimated the observed evaporation slope. Since regional δ^{18}O:δ^{2}H is better constrained than the timing of lake evaporation, the monthly humidity array is 'tuned' upward by a factor of 1.15 to match the modeled steady-state δ^{18}O:δ^{2}H relationship with the Ovando-area evaporation trend.

The intralake seasonal range in δ^{18}O values for the JL and EL simulations is very similar to field observations. Divergence in mean annual composition between the JL and EL simulations is somewhat greater than the observed interlake differences, primarily due to EL compositions exceeding Evans Lake by about 5‰. Simulated EL compositions are similar to those of Long Lake, the most isotopically evolved lake in the region (ESM 2). Our heuristic framework for examining lake isotopic sensitivity to groundwater boundaries thus looks generally like the

Ovando setting in seasonal $\delta^{18}O$ amplitude and in $\delta^{18}O$:$\delta^{2}H$ relations.

Seasonal inflows and outflows over 2 model years (simulation years 41 and 42, after both volume and isotopic composition achieve oscillatory steady state), are shown in Fig. 5. Direct precipitation and evaporative fluxes are very similar between the two simulations (which have nearly identical lake areas in their base case configurations). The base case monthly groundwater inflow for the EL model is slightly lower than the mean monthly precipitation flux. In the JL simulation, groundwater inflow is more than twice the direct precipitation flux, and annually averaged groundwater outflow is comparable to the evaporation flux. In the EL model, groundwater outflow is volumetrically trivial, though nonetheless significant to long-term solute balance through control of elevated lake salinity (Shapley et al. 2005).

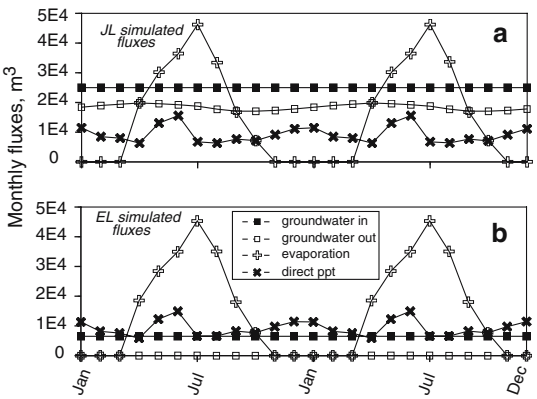

Fig. 5 Base case model fluid fluxes under steady-state conditions (**a**) High groundwater flux (JL; Jones Lake hypsometric model and groundwater influx). (**b**) Restricted groundwater flux (EL; Evans Lake hypsometric model and groundwater influx). Precipitation and evaporation fluxes (controlled by climate assumptions and lake surface areas) are very similar. In JL, groundwater inflow is proportionately higher than in EL. Groundwater outflow is an important flux in JL but volumetrically trivial in EL. Results are for model years 40 and 41, arbitrarily chosen to illustrate steady-state behavior following adjustment of initial assumed lake volumes to base case boundaries

Transient experiments I: modal fluid balance changes

We first examine the influence of groundwater setting on simulated lake response to simple step changes in independent model fluxes. These experiments assume base-case hydroclimatic conditions for 50 model years, allowing full isotopic adjustment from initial conditions. At year 51, the experimental conditions are changed instantaneously and maintained for the remainder of the 100 model-year simulation. Table 3 summarizes the experiments and the boundary condition changes made in each. Discussion of isotopic results is confined to $\delta^{18}O$; $\delta^{2}H$ results scale according to the model $\delta^{18}O$: $\delta^{2}H$ relationship shown in Fig. 4.

Table 3 Simulation parameters for model sensitivity experiments

Simulation	Duration (years)	Variables manipulated	Step time (years)	Omega (years)
BASE	100	None	None	None
PPT1	100	PPT = 0.85 BASE	50	None
PPT2	100	PPT = 0.70 BASE	50	None
PPT3	100	PPT = 0.55 BASE	50	None
PPT4	100	PPT = 0.40 BASE	50	None
GWIN1	100	GWIN = 0.83 BASE	50	None
GWIN2	100	GWIN = 0.66 BASE	50	None
GWIN3	100	GWIN = 0.49 BASE	50	None
EVAP4	100	EVAP = 1.354 BASE	50	None
GWINspring	100	GWIN biased (May–Jul) PPT = 0.7 BASE	50 (PPT)	30 (PPT)
SERIES1	500	PPT = 0.7 BASE GWIN = 0.83 BASE	250 (PPT, GWIN)	10 (PPT)
SERIES2	500	PPT = 0.7 BASE GWIN = 0.83 BASE	250 (PPT, GWIN)	20 (PPT)
SERIES3	500	PPT = 0.7 BASE GWIN = 0.83 BASE	250 (PPT, GWIN)	40 (PPT)
SERIES4	500	PPT = 0.7 BASE GWIN = 0.83 BASE	250 (PPT, GWIN)	60 (PPT)

Precipitation reduction

Experiments that progressively reduce annual precipitation while maintaining the base-case seasonal precipitation distribution are summarized in Fig. 6. Inherent in these simulations is the idea of proportionately increasing groundwater inflow as precipitation decreases. In the high groundwater-flux experiment (JL-PPT1), lake volume adjusts to reduced precipitation over about 6–8 years, declining in annually averaged lake volume to about 70% of the base case under the PPT*0.4 simulation. Sensitivity of isotopic composition is low; an initial transient increase in δ^{18}O values reaches only about 0.5‰ in the PPT*0.4 simulation. This small effect is rapidly reversed as the model approaches a new hydraulic steady state. At the end of the simulations, the reduced-PPT models have δ^{18}O values slightly lower than the base case.

In the low groundwater-flux/long residence-time experiment (EL-PPT1), modeled lake volume in the PPT*0.4 simulation declines to less than 40% of the base case. Initial transient response results in increases in δ^{18}O values reaching ca. 4‰ for the PPT*0.4 scenario. With the larger PPT perturbations (PPT*0.55 and PPT*0.4), the amplitude of the transient signal reaches or exceeds seasonal compositional variation (Fig. 6b). Several decades of declining mean annual δ^{18}O reflect an extended period of hydraulic equilibration in the EL model. Near-steady state wintertime values reached at the end of the simulations are lower than the base case, by almost 2‰ for the PPT*0.4 case. Summertime δ^{18}O values range from the base case value to ca. 1‰ lower.

Groundwater inflow reduction

Fluid balance adjustments driven by groundwater inflow changes (as would result from reduced aquifer recharge) should be expected to produce isotopic trajectories different those produced by

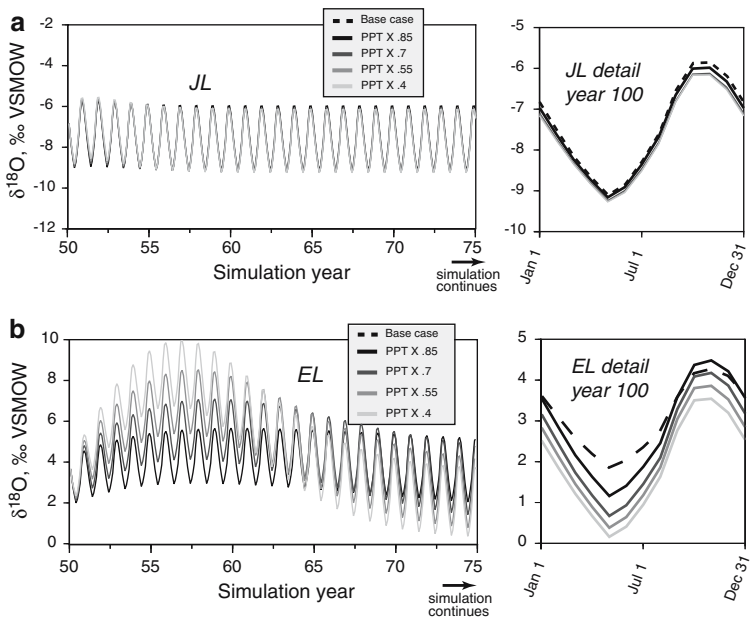

Fig. 6 δ^{18}O response to modal precipitation (PPT) reductions at simulation year 50; all other model parameters have the same seasonal distributions and annual totals before and after the modal change in PPT. Details are from simulation year 100, showing the steady-state seasonal compositional cycle following adjustment of lake volume and composition to perturbation. (**a**) Large groundwater fluxes minimize transient and steady-state compositional sensitivity in JL. (**b**) Evaporative outflow dominance under restrictive groundwater outflow conditions leads to a large transient increase in δ^{18}O values, followed by lowered steady-state δ^{18}O values and amplified seasonality as groundwater inflows increase in importance and lake volume declines

precipitation-driven changes. Results from experiments in which groundwater inflow was reduced by 17%, 34%, and 51% of base case values are summarized in Fig. 7. In the high groundwater-flux experiment (JL-GWIN), lake volume declines in approximate proportion to groundwater inflow, reaching a volume less than 50% of the base case under the 51% reduction. The initial transient rise in annually averaged δ^{18}O reaches about 2.5‰ above the base case. Steady-state δ^{18}O values at the end of the simulation remain slightly above the base case, by about 0.5‰ for the 51% reduction. The amplitude of the model's seasonal variation (more than 3‰) exceeds both the transient perturbation and the change in mean state.

For the low groundwater-flux/long residence-time experiment (EL-GWIN), lake volume is reduced to ca. 30% of the base case by a 51% reduction in groundwater inflow, causing a transient increase of up to 4.5‰ in δ^{18}O. Relaxation of the transient peak occurs over 30 years or more. At the end of the simulation, all EL-GWIN scenarios have returned to annual mean δ^{18}O values indistinguishable from the base case. However, the amplitude of the seasonal isotopic oscillation is increased symmetrically by about 1‰ in the case of the 51% reduction in GWIN. This effect is attributable to lake volume reduction disproportionately greater than inflow reduction; both winter inflow and summer evaporation act on a smaller reservoir, amplifying the isotopic effects of both fluxes.

Asymmetry of precipitation/evaporation fluxes

Sediment-based analyses of paleohydrology and paleoecology often invoke the concept of (precipitation–evaporation), or 'effective moisture', as a lumped climatic variable describing land-surface moisture conditions (e.g. Almendinger 1993). Implicit in this expression is the idea that the components of effective moisture act symmetrically; a unit reduction in average precipitation is

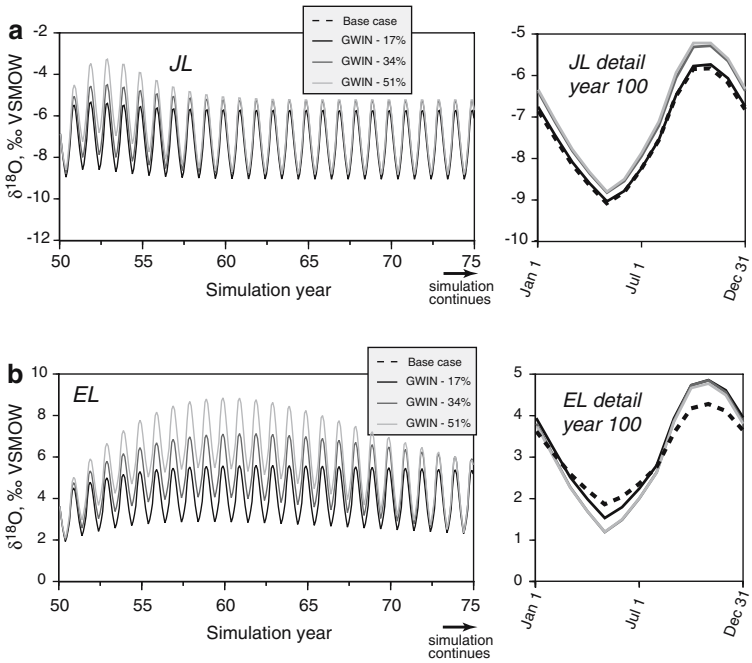

Fig. 7 δ^{18}O response to modal groundwater inflow (GWIN) reductions at simulation year 50; all other model parameters have the same seasonal distributions and annual totals before and after the modal changes in GWIN. Details are from simulation year 100, following adjustment of lake volume and composition to perturbation. (**a**) In JL, groundwater outflow results in short (ca. 5 year) transient effects, and a small increase in δ^{18}O values under steady-state conditions. (**b**) In EL, restricted groundwater outflow results in extended (>20 year) transient effects; the steady-state response is mainly in heightened seasonality of δ^{18}O due to reduced lake volume

equivalent to a unit increase in average evaporation. While a useful concept with respect to fluid balance, lake isotopic balances involving advected vapor and kinetic fractionation of lake water should not be expected to show such symmetry. The distinction between net fluid balance and isotope balance likely contributes to some instances of apparent disagreement between oxygen isotope records and other paleohydrologic indicators. The set of simulations summarized in Fig. 8 examines the influence of hydrogeologic setting on the expression of this asymmetry in evolving lake water. Figure 8a (JL-EVAP4) shows the response of the high groundwater-flux model to increasing annual evaporation rate by a factor of 1.35, equivalent in P–E terms to the PPT*0.4 decrease in precipitation rate used in the PPT-1 experiment; results from JL-PPT1 are shown for comparison. Annually averaged lake volumes (not shown) are nearly indistinguishable, while total annual volume variation is about 33% greater in the evaporation-forced case. Higher amplitude of seasonality in the increased evaporation simulation is driven by both higher (base case) winter precipitation flux and by increased evaporation flux during the open-water season. Under the enhanced evaporation forcing, JL-EVAP4 adjusts to δ^{18}O values 1–2‰ higher than JL-PPT1 throughout the year, with the difference maximized during the summer evaporation season.

In the EL system, which has relatively low groundwater inflow relative to precipitation and negligible groundwater outflow, volume differences between the precipitation and evaporation forcing scenarios are most prominent in the summer evaporation season (EL-EVAP4). Differences in δ^{18}O are minimal during the winter but reach ca. 1.5‰ during the summer evaporation season. In both JL and EL experiments, combinations of precipitation and evaporation rates with identical Δ (P–E) drive isotopic evolution of modeled lakes toward noticeably different mean composition and seasonal variability.

Transient experiments II: Oscillatory variation

To evaluate the effect of hydrogeologic setting on how lake isotopic composition responds to an oscillating climate, we now simulate cyclic long-term (>annual) change in hydroclimatic conditions. These experiments impose sinusoidal variation of various amplitude and frequency on precipitation. Amplitude of the oscillation is

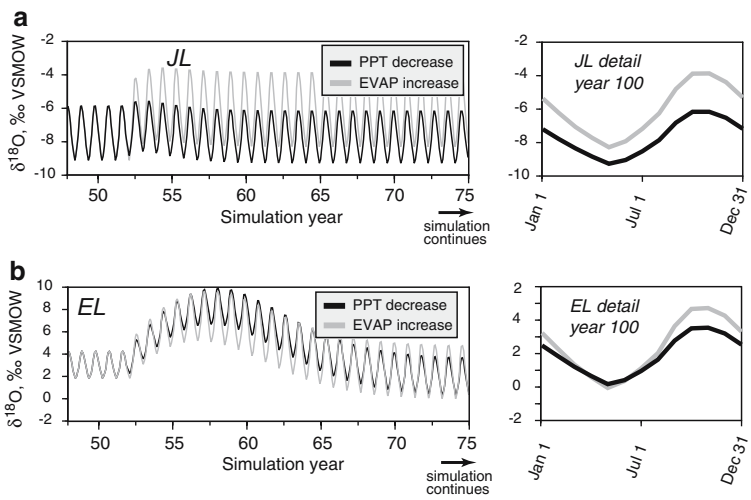

Fig. 8 Comparison of the δ^{18}O response to linearly equivalent precipitation (PPT) decrease and evaporation (EVAP) increase. PPT and EVAP experiments each result in reduction in net surface moisture availability of 0.26 m. (**a**) In JL, enhanced evaporation results in higher δ^{18}O values than precipitation reduction throughout the seasonal cycle. (**b**) In EL, enhanced evaporation results in higher δ^{18}O values than precipitation reduction during the evaporation season but late winter and spring compositions are indistinguishable

defined with respect to annual totals for the hydroclimatic variable. Seasonal distribution of the annual precipitation total remains unchanged from the base case.

Results of varying the period of the sinusoidal component in the high groundwater-flux setting (JO-OMEGA1; JO-OMEGA3) are shown in Fig. 9a. Precipitation rate is varied with amplitude of ±0.3 X the base case, on 10- and 30-year periods. The amplitude of modeled lake volume variation increases by about 30% when the forcing period increases over this range, reflecting incomplete approach to steady state inherent in oscillatory forcing. In both cases, the amplitude of interannual response exceeds the annual signal only modestly. Isotopic sensitivity is low (ca. 0.5‰), and the amplitude of δ^{18}O variation is indistinguishable between the two forcing periods.

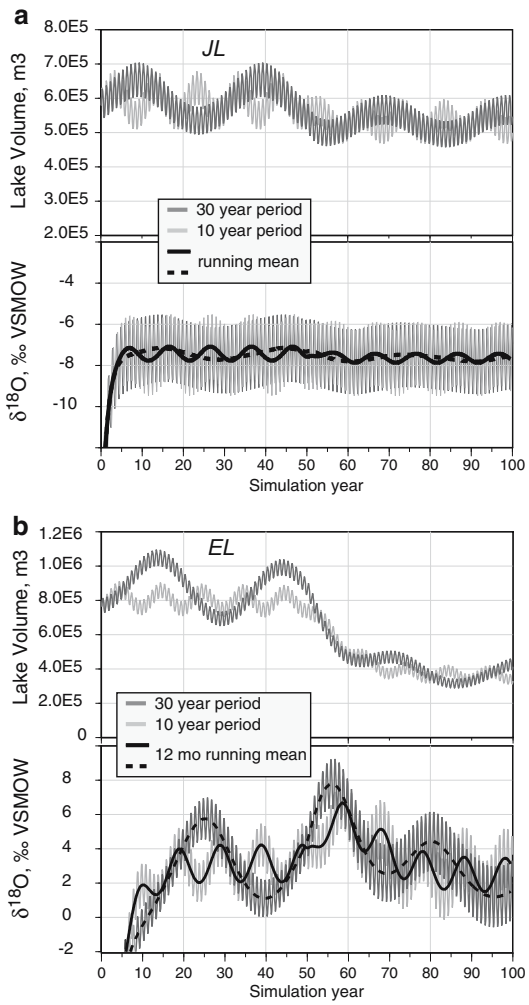

Fig. 9 Model lake volume and δ^{18}O response to combined modal reduction in PPT and oscillatory PPT forcing with periods of 10 and 30 years. Cyclic forcing of identical amplitude but differing period produces response of different amplitudes, The effect is subtle in JL (**a**) and is magnified in EL (**b**) due to longer residence time governed by restricted groundwater outflow

In the low groundwater-flux experiment (Fig. 9b) the volumetric response to the same precipitation forcing scenarios (EV-OMEGA1; EV-OMEGA3) results in a greater difference in volume response between the two forcing periods. Response of isotopic composition is similarly amplified, especially relative to the seasonal signal. Importantly, the amplitude of isotopic oscillation driven by the variable precipitation is sensitive to the *period* of forcing applied. Precipitation oscillation with period of 30 years results in 2.5‰ greater range in δ^{18}O than the same amplitude of forcing with a period of 10 years. This result suggests that a paleorecord from a restricted-outflow, long residence-time lake could show a change in δ^{18}O amplitude of several ‰ strictly as a consequence of changing period of forcing, with no change in amplitude of forcing.

Groundwater inflow seasonality

Simulations discussed up to this point incorporate a constant monthly rate of groundwater inflow. This assumption is inconsistent with the actual groundwater recharge and inflow timing in this region. Groundwater compositions sampled in the Ovando area are skewed toward lower, cold-season precipitation compositions. This probably results from preferential recharge of spring snowmelt prior to the seasonal increase in plant transpiration, as observed in other semiarid settings (Sophocleous and Perry 1985; Fritz et al. 1987). Seasonally biased recharge contributes in turn to transience in groundwater discharge to lakes and wetlands (Winter 1983; Rosenberry and Winter 1997).

Simulations summarized in Fig. 10 examine the sensitivity of our two lake models to seasonality in groundwater inflow rate. Here we assume groundwater composition identical to previous

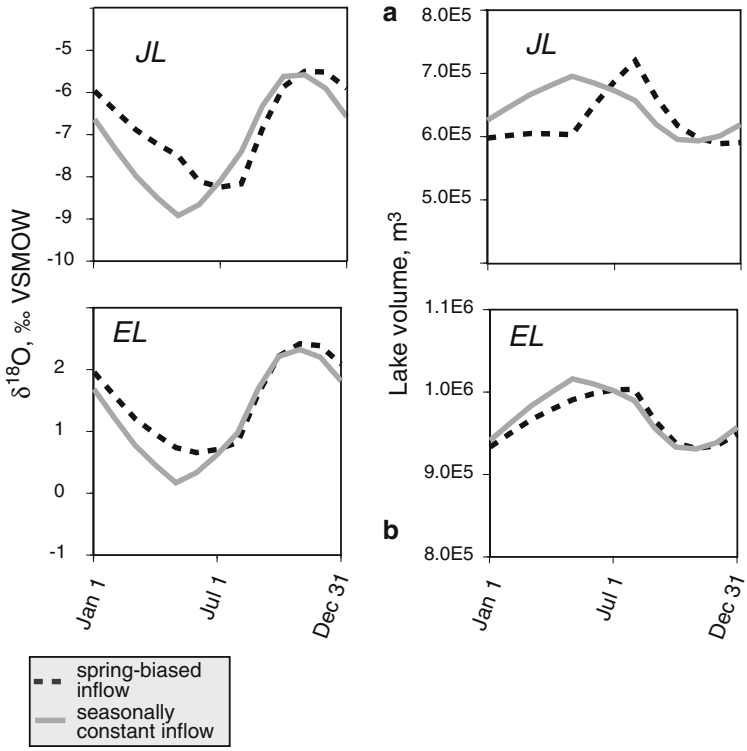

Fig. 10 Model lake volume and δ^{18}O response to a temporal shift in groundwater inflow. Spring-biased inflow assumes that 25% of total annual groundwater inflow occurs in each of the months April, May and June, with the remainder distributed evenly through the remaining months of the year. All other model parameters have the BASE seasonal distributions in both scenarios. Spring-biased inflow narrows the seasonal range of δ^{18}O, as inflow is moved into the period of active lake evaporation. The effect is controlled mainly by evaporation rate and inflow timing, and so looks similar in (**a**) JL, the high groundwater-flux case, and (**b**) EL, the restricted groundwater-flux case

simulations and simply redistribute the inflow seasonally. The experimental distribution of inflow is arbitrary but qualitatively plausible, assuming 75% of inflow occurs during April, May, and June. The remaining annual inflow is distributed evenly over the rest of the year. In the high groundwater-flux simulation (JL-GWINspring), maximum lake volume shifts from April to July and the amplitude of seasonal volume change is increased by about 5% relative to the constant-groundwater case (Fig. 10a). Most of the increased amplitude in volume is due to a higher early-summer peak volume resulting from the seasonally focused inflow. Reduced groundwater inflow during fall and winter months leads to a much smaller volume increase over this period than occurs in the base case. The response of δ^{18}O values to the spring-biased groundwater inflow is an increase approaching 1‰ in seasonal δ^{18}O minimum and equivalent decrease in the annual range of δ^{18}O. Most of the inflow occurs during months of relatively high evaporation, resulting in damping of the seasonal decline in δ^{18}O values and an upward shift of the seasonally averaged lake composition. Little change in the seasonal δ^{18}O maximum occurs.

In the low groundwater-flux simulation (EL-GWINspring) the amplitude of volume seasonality is reduced slightly (Fig. 10b), in contrast with the JL-GWINspring simulation. As with the JL simulation, the response in δ^{18}O values is a truncation in the seasonal minimum, as inflow is shifted into the evaporation season. In this case, the magnitude of the effect is noticeably greater after the modal change in precipitation occurring at year 50 (not shown), as lake volume declines dramatically and groundwater inflow becomes more important to lake isotope balance.

Discussion

Our results show several possible effects of hydrogeologic setting on the evolution of isotopic composition in lakes. Some elements of model response are attributable to groundwater processes or groundwater/lake interaction as implemented by model assumptions, while others result from differences in lake residence time, also controlled by groundwater inflow and outflow rates. Thus in either case, groundwater fluxes influence how prominently different climate effects are expressed in modeled lake water, and therefore how isotopic paleorecords may be expected to record hydroclimatic variation.

Changes in simulated groundwater inflow dominance occur when precipitation fluxes are reduced without proportional reduction of groundwater inflow. While complete decoupling of groundwater and precipitation inflows (as in the PPT1 simulation) is unlikely, increasing relative aquifer contribution to lakes is a plausible result of watershed aridification. Not surprisingly, where modeled groundwater inflows are initially high relative to incident precipitation, reduction of direct precipitation has less effect on weighted inflow composition and on outflow rate than where precipitation is an initially larger fluid balance component. As a result, the steady-state sensitivity shown by our high-flux model to large reductions in precipitation (up to 60%) does not exceed 0.5‰ under the assumption of constant groundwater composition. An isotopic response of this magnitude is not likely to be resolved with confidence in a lacustrine paleorecord. By contrast, our low groundwater-flux model shows steady-state sensitivity at the 1–2‰ level to the same precipitation forcing. Both models show declines in steady-state isotopic composition under reduced precipitation, following initial transient (and much larger) increases in $\delta^{18}O$ and $\delta^{2}H$ values occurring as lake storage comes into balance with new inflow conditions. A decline in δ values is an expected consequence of changing source dominance under our model assumptions, and is consistent with previous interpretations of water compositions (e.g. Gosselin et al. 1997) and isotopic paleorecords (e.g. Last et al. 1994; Smith et al. 2002) in some groundwater-influenced lakes. The resulting compositional record of aridification can be seen as counterintuitive if changing ratios of groundwater and precipitation are not considered.

High rates of groundwater outflow speed approach to a new hydraulic steady state following fluid balance perturbation. Therefore groundwater fluxes influence both the amplitude (through source composition control) and the duration (through residence time) of isotopic response to climate forcing. Compared to high groundwater flux scenarios, low groundwater flux scenarios show higher-amplitude response to modal climate change, in keeping with the understanding of long residence-time lakes as 'amplifiers' of hydroclimatic signals. In simulations of lake response to decreased precipitation, the upward transient component of isotopic response eventually gives way to steady-state compositions slightly lower than the base case, as lake volume adjusts and compositional influence of groundwater inflow increases.

In the low-flux (EL) model, following the initial transient rise in δ values, lake composition follows a relatively long-term *downward* trajectory that is the most sustained feature of model response to reduced fluid balance, whether occurring through reduction of precipitation or groundwater inflow. In a high-resolution lacustrine paleorecord, such a feature could be mistaken for a signal of progressively increasing moisture balance. Here the trend represents part of the system response to past decreased moisture balance and is not contemporaneous with any change in climate conditions.

By buffering lake composition and shortening residence time, high groundwater fluxes limit the transient sensitivity of model lake composition to climatic forcing. This results in high intra-annual variability relative to interannual and decadal signals under most JL (high groundwater flux; short residence-time) model conditions. Detection of high-resolution interannual signals in such a system will tend to be confounded, placing a premium on paleorecord selection and sampling strategies that can fully characterize seasonality. Changing seasonality of groundwater discharge may have counterintuitive isotopic signatures; simulations of a seasonally variable (likely more

realistic) groundwater inflow pattern resulted in *less* seasonal variation in $\delta^{18}O$ values relative to base case simulations.

Groundwater fluxes control lake residence time in these examples, and so control the departure of isotopic signals from synchrony with climate forcing. Forcing-to-signal peak lag times for JL and EL under a range of multidecadal periodic oscillations in precipitation rate (Table 3, SERIES1, 2, 3 and 4;) are summarized in Fig. 11. Temporal offset of the signal peak increases with period of forcing, increases with lake volume in a given hydrologic setting, and increases with lake residence time in interlake comparison. The amplification of hydroclimatic signals produced by the low-flux model comes at the expense of synchrony with forcing. This observation emphasizes that in a hydrogeologically heterogeneous setting, the advantages of paleorecord signal visibility conferred by a restricted-outflow setting need to be weighed against the greater inherent temporal precision of the less sensitive high-flux setting, where climate and lake chemistry are more likely to be in phase or nearly so.

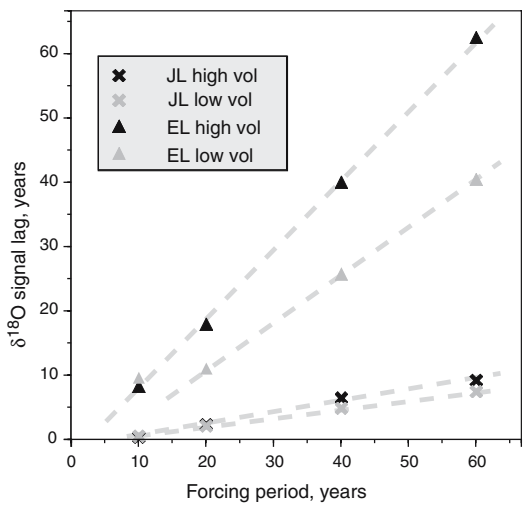

Fig. 11 $\delta^{18}O$ signal lag as a function of PPT forcing period in high groundwater- flux (JL) and restricted groundwater-flux (EL) settings. Results shown are from SERIES1, SERIES2, SERIES3 and SERIES4 with precipitation oscillations of period 10, 20, 40 and 60 years respectively. 'Low volume' results follow secular reductions in PPT and GWIN at simulation year 250. Signal lag is longer and increases more rapidly with forcing period in the restricted-flux (long residence time) model. Time lags are calculated as the cross-correlation offset between precipitation forcing (smoothed with a low-pass filter to remove seasonality) and the $\delta^{18}O$ signal

Conclusions

Transient isotope-balance modeling of evaporating lakes shows that hydrogeologic linkages can have a major influence on the sensitivity and spatial coherence of isotopic paleorecords. High ratios of modeled groundwater inflow to direct precipitation dampen steady-state lake sensitivity to changes in climate forcing through compositional buffering. High ratios of groundwater outflow to evaporation dampen lake sensitivity to climate forcing through rapid hydraulic adjustment to changing climatic boundaries, which reduces transient isotopic response. Depending on boundary conditions, prominent transient responses in lake isotopic composition may be opposite in sign to more subtle steady-state changes. Seasonal redistribution of modeled groundwater inflows, independent of change in total inflow or composition, alters the mean composition and seasonal range in lakes by changing the timing of water storage and the temporal relation of inflow to highly seasonal evaporation. Amplified sensitivity in restricted-outflow lakes, advantageous in bringing isotopic signal amplitude above seasonal variation and analytical noise, comes at the expense of temporal synchrony between forcing and signal.

These relationships have the potential to affect both the interlake coherence between isotopic paleorecords and the intra-lake coherence between isotopic composition and other proxy records of hydroclimate. Many observed complexities in spatial and temporal patterns of paleorecords may be due to one or more of the phenomena described here. Without explicit consideration of the effects of groundwater fluxes on lake residence time and inflow timing, isotope-based inferences regarding the magnitude, timing and spatial distribution of hydroclimatic excursions are likely to go astray.

Acknowledgements M.D.S. wishes to thank Lensyl Urbano for unfailingly generous assistance with Excel™ modeling applications. M.D.S. was supported in this work by University of Minnesota Department of Geology and Geophysics GeoFluids (NSF) and GAANN (U.S. Department of Education) fellowships. Invaluable support was also provided by the Minnesota Stable Isotope Lab and the Limnological Research Center LacCore Facility and their staffs. David Gosselin and Daniel Ariztegui provided helpful reviews resulting in an improved manuscript. This is LRC Contribution 07-1.

References

Almendinger JE (1993). A groundwater model to explain past lake levels at Parkers Prairie, Minnesota, USA. Holocene 3:105–115

Benson LV, Paillet F (2002). HIBAL: a hydrologic-isotopic-balance model for application to paleolake systems. Quat Sci Rev 21:1521–1539

Benson LV, White LD, Rye R (1996). Carbonate deposition, Pyramid Lake subbasin, Nevada: 4. Comparison of the stable isotope values of carbonate deposits (tufas) and the Lahontan lake-level record. Paleogeogr Paleoclimatol Paleoecol 122:45–76

Born SM, Smith SA, Stephenson DA (1979). Hydrogeology of glacial-terrain lakes, with management and planning applications. J Hydrol 43:7–43

Bowen GJ, Revenaugh J (2003). Interpolating the isotopic composition of modern meteoric precipitation. Water Resour Res 39(10): SWC9-1–SW9-13

Brenner M, Whitmore TJ, Riedinger-Whitmore MA, DeArmond B, Leeper DA, Kenney WF, Curtis JH, Shumate B (2006). Geochemical and biological consequences of groundwater augmentation in lakes of west-central Florida (USA). J Paleolimnol 36:371–383

Cook BJ (2001) Temporary hydrologic connections make 'isolated' wetlands function at the landscape scale. Ph.D. thesis, Division of Biological Sciences, Flathead Lake Biological Station, University of Montana, Missoula, 70 pp

Craig H, Gordon LI (1965) Deuterium and Oxygen 18 variations in the ocean and marine atmosphere. In: Tongiorgi E (ed) Stable isotopes in oceanographic studies and paleotemperatures. Laboratorio di Geologia Nucleare, Spoleto, Italy

Dea PA (1981) Glacial geology of the Ovando Valley, Powell County, Montana. M.S. thesis, Geology, University of Montana, Missoula, 107 pp

Dean WE, Forester RM, Bradbury JP (2002) Early Holocene change in atmospheric circulation in the Northern Great Plains: an upstream view of the 8.2 ka cold event. Quat Sci Rev 21:1763–1775

Dean WE, Stuiver M (1993) Stable carbon and oxygen isotope studies of the sediments of Elk Lake, Minnesota. In: Bradbury JP, Dean WE (eds) Elk Lake, Minnesota: evidence for rapid climate change in the North-Central United States. United States Geologic Survey. USGS Special Paper 276, Boulder, CO

Donovan JJ (1992) Geochemical and hydrologic dynamic in evaporative groundwater-dominated lakes of glaciated Montana and North Dakota. Ph.D. thesis, Pennsylvania State University, 251 pp

Donovan JJ (1994) Modeling chemical response of groundwater-dominated lakes to fluctuations in climate. In: Siriwardane HJ, Zaman MM. (eds), Eighth International Conference on computer methods and advances in geomechanics, Morgantown, WV

Donovan JJ, Smith AJ, Panek VA, Engstrom DR, Ito E (2002) Climate-driven hydrologic transients in lake sediment records: calibration of groundwater conditions using 20th Century drought. Quat Sci Rev 21:605–624

Epstein S, Mayeda T (1953) Variations of the $^{18}O/^{16}O$ ratio in natural waters. Geochim Cosmochim Acta 4:213–224

Fritz P, Drimmie RJ, Frape SK, O'Shea K (1987) The isotopic composition of precipitation and groundwater in Canada. In Isotope techniques in water resources development: proceedings of an international symposium on the use of isotope techniques in water resources development, Vienna, Austria

Gat JR (1995) Stable isotopes in fresh and saline lakes. In: Lerman A, Imboden DM, Gat JR (eds) Physics and chemistry of lakes. Springer-Verlag. Berlin, p 334

Gonfiantini R (1986) Environmental isotopes in lake studies. In: Fritz P, Fontes JC (eds) Handbook of environmental geochemistry, vol 2, The terrestrial environment, B. Elsevier Science Publishing Company, Inc., Amsterdam, p 557

Gosselin DC, Nabelek PE, Peterman ZE, Sibray S (1997) A reconnaissance study of oxygen, hydrogen and strontium isotopes in geochemically diverse lakes, Western Nebraska, USA. J Paleolimnol 17:51–65

Ito E (2001) Application of stable isotope techniques to inorganic and biogenic carbonates. In: Last WM, Smol JP (eds) Tracking environmental change using lake sediments, vol 2: physical and chemical techniques. Kluwer Academic Publishers. Dordrecht, The Netherlands, pp 351–371

Kendall C, Coplen T (1985) Multi-sample conversion of water to hydrogen by zinc for stable isotope analysis. Anal Chem 57:1437–1440

Krabbenhoft DP, Anderson MP, Bowser CJ, Valley JW (1990) Estimating groundwater exchange with lakes: 1) The stable isotope mass balance method. Water Resour Res 26:2445–2453

Last WM (2001) Mineralogical analysis of lake sediments. In: Last WM, Smol JP (eds) Tracking environmental change using lake sediments, vol 2: physical and chemical techniques. Kluwer Academic Publishers, Dordrecht, The Netherlands, pp 143–188

Last WM, Teller JT, Forester RM (1994) Paleohydrology and paleochemistry of Lake Manitoba, Canada: the isotope and ostracode records. J Paleolimnol 12:269–282

Majoube M (1971) Fractionnment en oxygene-18 et en deuterium entre l'eau et sa vapeur. J Chem Phys 197:1423–1436

MAPS Montana Agricultural Potentials System Atlas (2003) http://www.montana.edu/places/maps/. Accessed December 12, 2003

Merlivat L, Jouzel J (1979) Global climatic interpretation of the deuterium-oxygen 18 relationship for precipitation. J Geophys Res 84(C8):5029–5033

Rosenberry DO, Winter TC (1997) Dynamics of water-table fluctuations in an upland between two prairie-pothole wetlands in North Dakota. J Hydrol 191:266–289

Sanford WE, Wood W (1991) Brine evolution and mineral deposition in hydrologically open evaporite basins. Am J Sci 291:687–710

Schettler G, Liu Q, Mingram J, Negendank JFW (2006) Palaeovariations in the East-Asian monsoon regime geochemically recorded in varved sediments of Lake Sihailongwan (Northeast China, Jilin Province). Part 1: Hydrologic conditions and dust flux. J Paleolimnol 35:239–270

Shapley M, Ito E, Donovan JJ (2005) Authigenic calcium carbonate flux in groundwater-controlled lakes: implications for lacustrine paleoclimate records. Geochim Cosmochim Acta 69:2517–2533

Smith AJ, Donovan JJ, Ito E, Engstrom DR (1997) Groundwater processes controlling a prairie lake's response to middle Holocene drought. Geology 25:391–394

Smith AJ, Donovan JJ, Ito E, Engstrom DR, Panek VA (2002) Climate-driven hydrologic transients in lake sediment records: multiproxy records of mid-Holocene drought. Quat Sci Rev 21:625–646

Sophocleous M, Perry CA (1985) Experimental studies in natural groundwater-recharge dynamics: the analysis of observed recharge events. J Hydrol 81:297–332

Walker JF, Krabbenhoft DP (1998) Groundwater and surface-water interactions in riparian lake-dominated systems. In: Kendall C, McDonnell JJ (eds) Isotope tracers in catchment hydrology. Elsevier Science. Amsterdam, pp 467–488

Winter TC (1983) The interaction of lakes with variably saturated porous media. Water Resour Res 19:1203–1218

Winter TC, Labaugh JW, Rosenberry DO (1988) The design and use of a hydraulic potentiomanometer for direct measurements of differences in hydraulic head between groundwater and surface water. Limnol Oceanogr 33:1209–1213

Yu Z, Ito E, Engstrom DR (2002) Water isotopic and hydrochemical evolution of a lake chain in the Northern Great Plains and its Paleoclimatic implications. J Paleolimnol 28:207–217